

**Determination of the Ehrlich-Schwoebel barrier in epitaxial growth of thin films**

Shao-Chun Li

*Institute of Physics, Chinese Academy of Sciences, Beijing 100080, China*

Y. Han

*Department of Materials Science and Engineering, University of Utah, Salt Lake City, Utah 84112, USA*

Jin-Feng Jia

*Institute of Physics, Chinese Academy of Sciences, Beijing 100080, China*

Qi-Kun Xue

*Institute of Physics, Chinese Academy of Sciences, Beijing 100080, China  
and ICQS, Chinese Academy of Sciences, Beijing 100080, China*

Feng Liu

*Department of Materials Science and Engineering, University of Utah, Salt Lake City, Utah 84112, USA  
and ICQS, Chinese Academy of Sciences, Beijing 100080, China*

(Received 30 December 2005; revised manuscript received 27 September 2006; published 22 November 2006)

We demonstrate an approach for determining the “effective” Ehrlich-Schwoebel (ES) step-edge barrier, an important kinetic constant to control the interlayer mass transport in epitaxial growth of thin films. The approach exploits the rate difference between the growth and/or decay of an adatom and a vacancy two-dimensional island, which allows the “effective” ES barrier to be determined uniquely by fitting with a single parameter. Application to growth of Pb islands produces an effective ES barrier of  $\sim 83 \pm 10$  meV on Pb(111) surface at room temperature.

DOI: [10.1103/PhysRevB.74.195428](https://doi.org/10.1103/PhysRevB.74.195428)

PACS number(s): 68.35.Fx, 07.79.Cz, 68.35.Md, 68.65.-k

Epitaxial growth process is the mainstream method for producing high quality thin film materials with a control of single-atomic-layer precision. In general, the growth process, and hence the quality of the thin films, is controlled by the competition between growth thermodynamics and kinetics.<sup>1,2</sup> Consequently, there has been continued efforts<sup>3-14</sup> in developing effective methods for the determination of the thermodynamic and kinetic growth parameters. However, despite the notable progress we have made so far, the determination of the fundamental surface-growth constants remains often a difficult task. This is because these fundamental constants are generally not directly measurable.

Various approaches have been proposed for determining different thermodynamic and kinetic growth parameters. For example, surface step energy has been determined from measurement of surface step fluctuation<sup>3-6</sup> or from equilibrium shape of two-dimensional (2D) islands;<sup>5,7,8</sup> surface diffusion barrier from nucleation density of 2D islands;<sup>9,10</sup> and Ehrlich-Schwoebel (ES) step-edge barrier<sup>15,16</sup> from island nucleation density on top of an island<sup>11-13</sup> or from decay of stepped mounds.<sup>14</sup> In all the cases,<sup>3-14</sup> the constants are determined indirectly, by experimental measurements in combination with theoretical modeling and fitting, assuming that certain surface and growth morphological manifestation is controlled by the targeted growth constants. However, these approaches may suffer from the drawback that different theoretical models and multiple parameters are involved in the actual growth process and fitting procedure, causing ambiguity. For example, rather different ES barriers have been derived from the same set of experiments using different models of island nucleation theory.<sup>11-13</sup> Therefore, it is highly

desirable to develop effective approaches for determining surface-growth parameters that involves theoretical models as simple as possible and fitting parameters as few as possible.

There are two most important kinetic energy parameters involved in epitaxial growth of multilayer films, i.e., the surface diffusion barrier and the ES step edge barrier. The former controls the intralayer mass transport and the latter controls the interlayer mass transport. The ES barrier represents the extra energy barrier for an adatom descending over a step edge (i.e., transport from one atomic layer to another); its existence is ubiquitous in surface growth process, which is generally mediated by step creation and/or annihilation and motion. Yet, an accurate experimental determination of the ES barrier is rather difficult, because it generally involves growth of multilayer morphology.<sup>14</sup> (In contrast, determination of surface diffusion barrier involves only single-layer growth.<sup>9,10</sup>) This has complicated the theoretical modeling and fitting procedure.<sup>11-14</sup>

Here, we demonstrate an approach for the experimental determination of the ES barrier, which may have some advantages over the previous approaches. It is based on exploiting a simple manifestation of the ES barrier, the difference between the decay rate of a 2D vacancy island and the growth rate of a 2D adatom island, which were measured under identical conditions. Consequently, it involves a “deterministic” growth process of only one 2D island rather than a stochastic nucleation process of many islands.<sup>11-13</sup> Also, by taking the difference between the growth rate of a 2D adatom island and the decay rate of 2D vacancy island, one can uniquely determine the ES barrier by theoretically fitting the

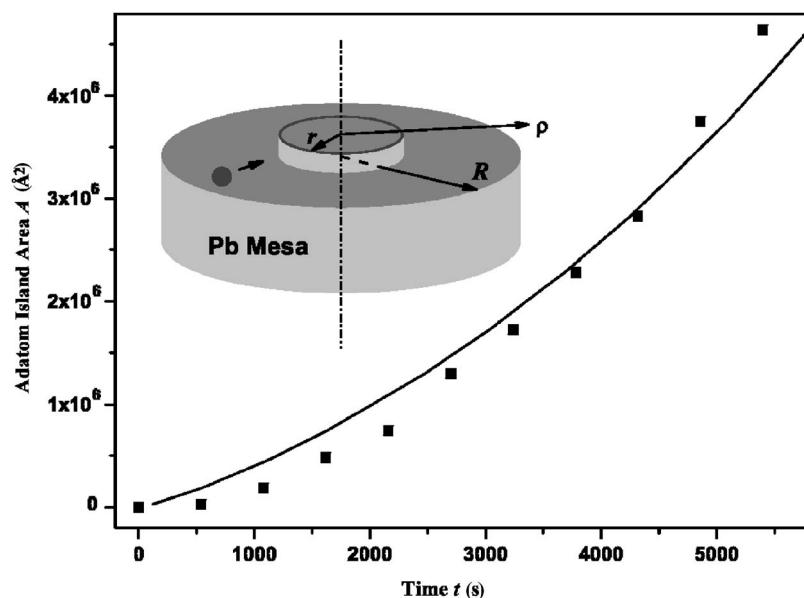


FIG. 1. The area of an adatom island grown on a mesa top as a function of time. Squares are experimental data and the line is the theoretical fit using Eq. (4). Inset, schematic illustration denoting the adatom island and mesa geometry.

experiments with a single parameter rather than several parameters involved in many other approaches.

It is worth noting that surface diffusion barrier is a constant independent of temperature, while the ES barrier, in contrast, depends generally on temperature because temperature can change step structures which in turn changes the ES barrier. This point, which has been somewhat overlooked in the previous studies, makes the determination of the ES barrier even more complex. Specifically, in growth of 2D islands, the island step edge consists of segments of different step orientations and kinks, and their relative concentration is a function of temperature, i.e., the 2D island will take different shape at different temperature. In general, the energy barriers for an adatom descending over different orientations of step segments and over kinks are different. Consequently, what has been measured is an “effective” ES barrier, corresponding to a particular step configuration at the given temperature, averaged over different descending processes. In the present work, we have applied our approach to the growth and/or decay of Pb 2D islands, which allowed us to determine the effective ES barrier on Pb(111) surface to be  $\sim 83 \pm 10$  meV at room temperature.

Let us introduce the basic idea of the approach. Consider first the growth of a 2D adatom island on a cylindrical mesa top of radius  $R$ , as shown by the inset of Fig. 1. (The experimental realization of such a process is discussed below.) For isotropic step energies, the island adopts a circular shape with radius  $r$  at time  $t$ . Solving the adatom surface diffusion equation, one easily obtains the steady-state adatom concentration on the terrace (mesa top) between the island edge and the mesa edge as

$$n(\rho) = C_1 + C_2 \ln \rho, \quad (1)$$

where  $n(\rho)$  is the adatom concentration in polar coordinates;  $C_1$  and  $C_2$  are the constants to be determined by the boundary conditions. Assuming the island step edge acting as a perfect sink (see discussion below), the adatom concentration next to the growing island is zero, i.e., at the island edge,

$n_b = 0$ . At the mesa edge, far away from the growing island, the adatom concentration,  $n(\rho=R) = n_R$  is equal to the equilibrium surface adatom concentration. Then we have  $C_2 = \frac{n_R}{\ln(R/r)}$ .

The growth rate of the adatom island is proportional to the negative adatom flux ( $J$ ) at  $r$ , i.e.,

$$\frac{1}{\Omega} \frac{dr}{dt} = -J = D \left. \frac{dn}{d\rho} \right|_{\rho=r}, \quad (2)$$

where  $\Omega$  is the atomic area (area per atom) in the island and  $D$  is the surface diffusion coefficient. Integrating Eq. (2), we obtain

$$r^2 \ln \frac{e^{1/2} R}{r} = 2\alpha t, \quad (3)$$

and  $\alpha = \Omega D n_R$ . In terms of the area of adatom island ( $A = \pi r^2$ ), we have

$$A \ln \frac{\pi R^2 e}{A} = 4\pi \alpha t. \quad (4)$$

Therefore, the growth rate of adatom island is controlled by a single parameter  $\alpha$ , which is related to surface diffusion coefficient and equilibrium surface adatom concentration.

Next, we consider the decay of a 2D vacancy island on the same cylindrical mesa top, as shown by the inset of Fig. 2. In comparison with the adatom island, the main difference is that the adatom encounters an additional ES barrier ( $\Delta$ ) before incorporating into the vacancy island edge (see the inset in Fig. 2). This modifies the boundary condition at the vacancy island edge as<sup>17</sup>

$$\left. \frac{dn(\rho)}{d\rho} \right|_{\rho=r} = \frac{n(r) - n_b}{l_{ES}}, \quad (5)$$

where parameter  $l_{ES} = a_0(e^{\Delta/kT} - 1)$  represents effectively an extra distance that an adatom must jump over the step in the presence of the ES barrier,  $a_0$  is the surface lattice constant,

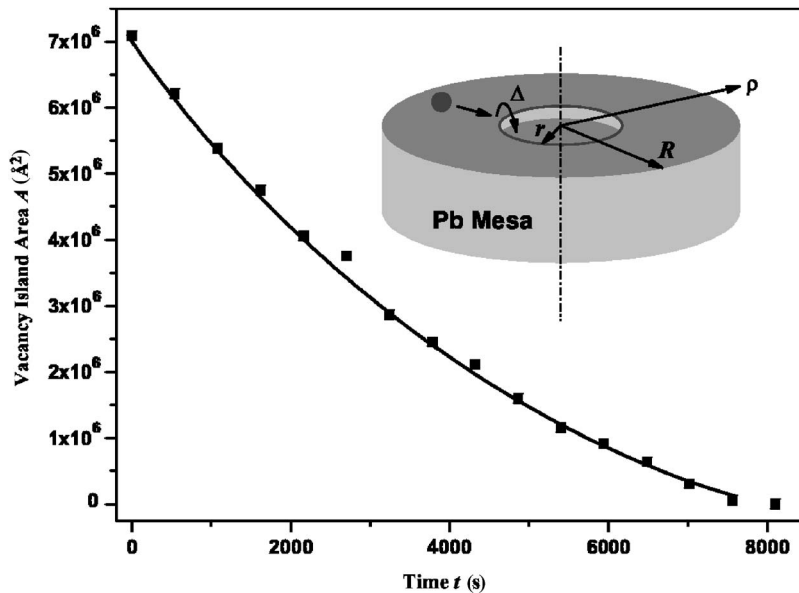


FIG. 2. The area of a vacancy island grown on a mesa top as a function of time. Squares are experimental data and the line is the theoretical fitting using Eq. (8). Inset, schematic illustration denoting the vacancy island and mesa geometry.

and  $n_b$  is the equilibrium density at the vacancy island boundary (the step bottom), which would be zero for a boundary acts as a perfect sink. We solve the decay rate of the vacancy island, which is proportional to the adatom flux, as

$$\frac{1}{\Omega} \frac{dr}{dt} = J = -D \left. \frac{dn}{d\rho} \right|_{\rho=r}, \quad (6)$$

$$C_s - 2r l_{ES} - r^2 \ln \frac{e^{1/2} R}{r} = 2\alpha t, \quad (7)$$

$$2\pi C_s - 4\pi l_{ES} \sqrt{A/\pi} - A \ln \frac{\pi R^2 e}{A} = 4\pi\alpha t, \quad (8)$$

where  $C_s = 2r_s l_{ES} + r_s^2 \ln(e^{1/2} R/r_s)$ , and  $r_s$  is the starting vacancy island radius (see the experiments below).  $A$  is now the area of the vacancy island at time  $t$ .

Comparing Eqs. (4) and (8), we can see that in addition to the parameter  $\alpha$ , the decay rate of the vacancy island is further controlled by the parameter  $l_{ES}$ . In essence, the growth rate of the 2D island is controlled by a single kinetic parameter of surface diffusion energy barrier, while the decay rate of a 2D vacancy island is controlled by one additional kinetic parameter of ES barrier. Thus, by simultaneously measuring

the decay rate of a vacancy island vs the growth rate of an adatom island under identical condition, the ES barrier can be uniquely determined by a single-parameter fitting to Eq. (8) following the fitting to Eq. (4). Below, we demonstrate an experimental procedure to realize such an approach on Pb(111) surface.

The experiments are performed with an OMICRON variable-temperature STM under ultrahigh vacuum ( $\sim 1.0 \times 10^{-10}$  Torr).<sup>18-20</sup> The Si(111)-(7×7) substrate used is cleaned by several times of flash annealing up to 1000 °C. High purity Pb (99.999%) is thermally evaporated from the resistive heated tungsten boat. The deposition rate is regulated to be about 0.5 monolayer (ML) per minute. STM images are acquired under the constant current mode with typical tunneling current 0.02 nA and bias voltage 0.5 V–2.0 V.

First, the flat-top Pb mesas are created on Si(111) substrate, as described before.<sup>18,19</sup> Briefly, several MLs of Pb are deposited on the clean Si(111)-(7×7) surface held at room temperature, and the Pb islands grow on the wetting layer following the Stranski-Krastanov mode. Using the STM manipulation process,<sup>18,19</sup> we construct a mesa-shaped flat-top Pb island, as shown in Fig. 3(a); the mesa height is about 60 ML.

Next, we induce nucleation and growth of a monolayer adatom island by applying an STM pulse on the mesa top, as

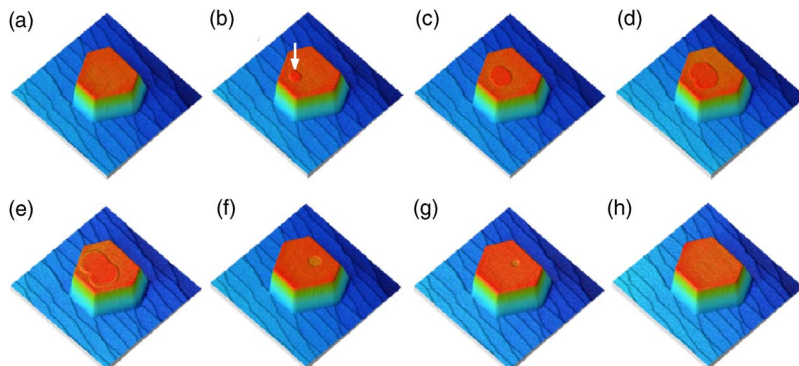


FIG. 3. (Color online) STM images (720 nm×720 nm) recording the growth of the monolayer-height adatom and vacancy islands on top of a Pb mesa formed on the Si(111)-(7×7) surface. (b)–(d) Images of adatom island. (f)–(h) Images of vacancy island.

shown in Fig. 3. The pulse is placed off the center of the mesa top [see Fig. 3(b)], so an adatom island nucleates and grows first in a circular shape [Figs. 3(b)–3(d)]. Because the adatom island is located off the center, one of its side will hit the mesa edge and the island then becomes distorted (anisotropic) [Fig. 3(e)]. As soon as this happens, however, it will rapidly spread around the mesa edge into a complete loop, forming a vacancy island in a circular shape [Fig. 3(f)] that will continue to decay and disappear<sup>18</sup> [Fig. 3(h)]. In this way, we can sequentially record first the growth rate of an adatom island [Figs. 3(b)–3(d) when it remains circular before hitting the edge] and then the decay rate of a vacancy island [Figs. 3(f)–3(h) when it remains circular] in one experimental setting, to facilitate an accurate comparison.

We note that we have used a rather unique and nonconventional experimental setup, in which the nucleation and growth of an adatom island followed by the decay of a vacancy island on the Pb mesa top can only be triggered by an STM pulse. In the conventional coarsening process, the chemical potential of a 2D island is inversely proportional to its radius  $R$  due to curvature effect, i.e., the step energy is proportional to its curvature ( $1/R$ ). Consequently, a small island should decay by dissolving adatoms to larger islands or surface steps. However, in our special setup, the small adatom island on the mesa top is nucleated by applying a STM pulse, so that it is temporarily charged with  $Q$ . The Coulomb charging greatly reduces the chemical potential of the island by the amount of  $Q^2/R^2$ . Such “Coulomb sink” effect<sup>19,21</sup> can make the chemical potential of a charged small island much lower than those of neutral large islands and straight steps, as Coulomb energy dominates over the step energy. This is the reason for the observed unconventional growth (instead of decay) of the adatom island, because its chemical potential is much lower than the surroundings due to the Coulomb sink effect, making it act effectively as a sink for adatoms. The Coulomb sink effect decreases with time because of charge leakage,<sup>19</sup> and by the time the adatom island converts to a vacancy island, the vacancy island can decay in the conventional manner even without charge.

The STM movies were recorded for the whole growth and/or decay process (for both adatom and vacancy island) with a time interval of  $\sim 8$  minutes and some snap-shots are shown in Fig. 3. For both the adatom and vacancy island, the growth fronts keep a nearly circular shape except when the adatom island just hits the mesa edge [Fig. 3(e)]. The shape of the Pb mesa remains unchanged, indicating the growth was facilitated by Pb atoms from the surroundings. The areas of islands are calculated from the STM images after software calibration. Figures 1 and 2 show the measured temporal evolution of the area of the adatom island and the vacancy island, respectively. It is then straightforward to fit the experimental data (square dots) with the theoretical model discussed above.

First, we fit the growth rate of the adatom island using Eq. (4), as shown in Fig. 1. The experimental setup is not ideal; the Pb mesa top actually has a distorted hexagonal shape, which was replaced with a circle of radius  $R=2500$  Å; also the adatom island was located off the center of the mesa. Considering these approximations and the fact that only one fitting parameter,  $\alpha$ , was involved, the fitting curve to the

experimental data is rather impressive. This indicates that the theoretical model likely gives a reasonably correct representation (functional form) of the measured growth rate. The resulting parameter  $\alpha=155\pm 15$  Å<sup>2</sup>/s. The error bars reflect partly the above-mentioned approximations.

From the fitted value of  $\alpha$ , we can do some simple estimation of the adatom diffusion barrier and the adatom formation energy. For example, using the embedded-atom-method (EAM), we calculated a surface diffusion barrier of  $\sim 45$  meV,<sup>22</sup> while the experimental estimate is  $\sim 100$  meV.<sup>23</sup> Using these two values as the upper and lower bound, we obtain the adatom formation energy in the range of 0.67 eV–0.73 eV, which agrees well with 0.8 eV as estimated by Thürmer *et al.*<sup>6</sup> The good agreement further validates quantitatively our theoretical model and approach.

Next, we fit the decay rate of the vacancy island using Eq. (8), as shown in Fig. 2. Because the parameter  $\alpha$  is already known from the fitting of the adatom island, once again the whole fitting involves only one single parameter  $l_{ES}$ . The fitting matches experimental data perfectly, as shown in Fig. 2. Using a surface lattice constant of  $a_0=3.5$  Å and the starting vacancy island radius  $r_s=1500$  Å, we obtain from the fit the ES barrier  $\Delta\sim 83\pm 10$  meV. We note that this value is derived by fitting the theoretical model to multiple experimental data of decay rate in time scale at single growth temperature of 300 K, which has an error of about  $\pm 10$  K.

We emphasize that what we measured here is an “effective” ES barrier at the boundary (step edge) of a Pb(111) 2D vacancy island, which remains a circular shape throughout the measurement at the given room temperature of growth. The circular shape means the island step edge is nonfaceted, consisting of a mixture of many small segments of Pb(111) *A*-type and *B*-type steps<sup>24</sup> and corners (kinks) in between. This is consistent with the very low melting temperature of Pb, so that at room temperature (about one-half of the melting point) the island step edge is already roughened creating many kinks (in an analogy to surface roughening with creation of steps). Indeed, at lower temperatures, we observed that the island step edge is faceted and the island adopts a hexagonal shape consisting of straight *A*-type and *B*-type steps with few corners. Therefore, the experimentally measured “effective” ES barrier at room temperature should reflect the average barrier for adatom descending over *A*-type and *B*-type steps and over the kinks, as the barrier for each of these processes is different. Our EAM calculations<sup>22</sup> have shown that an adatom jumps over an *A*-type step via a rolling-over motion having a barrier of 100 meV, but over a *B*-type step via a concerted motion having a smaller barrier of 30 meV. The experimentally measured average value, which falls in between these EAM calculated ES barriers, appears reasonable.

In a previous experiment,<sup>18</sup> only the decay of vacancy island was observed and speculated to be mediated via surface vacancy diffusion. In the present experiment, however, by observing the adatom island growth and the vacancy island decay under the same condition, it becomes clear the two processes are most likely mediated by the same surface diffusion mechanism except there is an additional ES barrier for the vacancy island decay. This is reflected by the good

fitting with the same parameter  $\alpha$  (or diffusion coefficient) for both processes. In contrast, the surface diffusion coefficient is expected to be different between an adatom and a vacancy. Since the adatom island must grow via adatom diffusion, it is then likely the vacancy island decays also via adatom diffusion.

Although we have used a unique (nonconventional) process, in which the adatom island grows while the vacancy island decays, the rate difference between an adatom and a vacancy island, nevertheless, should still reflect the effect and magnitude of the ES barrier for either growth or decay. Therefore, the approach we introduce here is generally applicable for the determination of the ES barrier as long as a quantitative comparison of growth or decay rate can be made between an adatom and a vacancy island, by different innovative experimental setup. Also, noting the fact that the ES barrier is generally a function of temperature, our approach has happened to provide a convenient way to measure the effective ES barrier at a given temperature, because it is

based on the growth and/or decay rate difference between an adatom and a vacancy island at the same temperature.

In conclusion, we have demonstrated a simple and effective approach for experimental determination of the effective ES barrier, one of the key kinetic parameters involved in the surface growth process. The approach exploits the rate difference between the growth and/or decay of an adatom and a vacancy island, which uniquely manifests the effect and magnitude of the ES barrier. This approach has the distinct advantages involving simple theoretical modeling with only one-parameter fitting. It should be generally applicable to other systems. We have applied this approach to Pb(111) surface and obtained an effective ES barrier to be  $\sim 83$  meV at room temperature.

The work at Utah is supported by NSF (Grant No. DMR-0307000). The work at Beijing is supported by National Science Foundation of China, and Ministry of Science and Technology of China.

- 
- <sup>1</sup>F. Liu, F. Wu, and M. G. Lagally, *Chem. Rev.* (Washington, D.C.) **97**, 1045 (1997).
- <sup>2</sup>F. Liu and M. G. Lagally, *Surf. Sci.* **386**, 169 (1997).
- <sup>3</sup>B. S. Swartzentruber, Y.-W. Mo, R. Kariotis, M. G. Lagally, and M. B. Webb, *Phys. Rev. Lett.* **65**, 1913 (1990).
- <sup>4</sup>H. J. W. Zandvliet, H. B. Elswijk, E. J. van Loenen, and D. Dijkkamp, *Phys. Rev. B* **45**, 5965 (1994).
- <sup>5</sup>N. C. Bartelt, R. M. Tromp, and E. D. Williams, *Phys. Rev. Lett.* **73**, 1656 (1994).
- <sup>6</sup>K. Thürmer, J. E. Reutt-Robey, E. D. Williams, M. Uwaha, A. Emundts, and H. P. Bonzel, *Phys. Rev. Lett.* **87**, 186102 (2001).
- <sup>7</sup>A. Li, F. Liu, and M. G. Lagally, *Phys. Rev. Lett.* **85**, 1922 (2000).
- <sup>8</sup>V. Zielasek, F. Liu, Y. Zhao, J. B. Maxson, and M. G. Lagally, *Phys. Rev. B* **64**, 201320(R) (2001).
- <sup>9</sup>Y. W. Mo, J. Kleiner, M. B. Webb, and M. G. Lagally, *Phys. Rev. Lett.* **66**, 1998 (1991).
- <sup>10</sup>F. Liu and M. G. Lagally, in *The Chemical Physics of Solid Surfaces*, edited by D. A. King and D. P. Woodruff (Elsevier, Amsterdam, 1997), Vol. 8, p. 258.
- <sup>11</sup>K. Bromann, H. Brune, H. Röder, and K. Kern, *Phys. Rev. Lett.* **75**, 677 (1995).
- <sup>12</sup>J. Tersoff, A. W. Denier van der Gon, and R. M. Tromp, *Phys. Rev. Lett.* **72**, 266 (1994).
- <sup>13</sup>J. Krug, P. Politi, and T. Michely, *Phys. Rev. B* **61**, 14037 (2000).
- <sup>14</sup>M. Giesen and H. Ibach, *Surf. Sci.* **431**, 109 (1999).
- <sup>15</sup>G. Ehrlich and F. G. Hudda, *J. Chem. Phys.* **44**, 1039 (1966).
- <sup>16</sup>R. L. Schwoebel and E. J. Shipsey, *J. Appl. Phys.* **37**, 3682 (1966).
- <sup>17</sup>G. S. Bales and A. Zangwill, *Phys. Rev. B* **41**, 5500 (1990).
- <sup>18</sup>C.-S. Jiang, S. C. Li, H. B. Yu, D. Eom, X. D. Wang, P. Ebert, J. F. Jia, Q. K. Xue, and C. K. Shih, *Phys. Rev. Lett.* **92**, 106104 (2004).
- <sup>19</sup>Y. Han, J. Y. Zhu, F. Liu, S. C. Li, J. F. Jia, Y. F. Zhang, and Q. K. Xue, *Phys. Rev. Lett.* **93**, 106102 (2004).
- <sup>20</sup>S.-C. Li, J. F. Jia, R. F. Dou, Q. K. Xue, I. G. Batyrev, and S. B. Zhang, *Phys. Rev. Lett.* **93**, 116103 (2004).
- <sup>21</sup>S.-C. Li, J.-F. Jia, X. Ma, Q.-K. Xue, Y. Han, and F. Liu, *Appl. Phys. Lett.* **89**, 123111 (2006).
- <sup>22</sup>Y. Han and F. Liu (unpublished).
- <sup>23</sup>K. Arenhold, S. Surnev, H. P. Bonzel, and P. Wynblatt, *Surf. Sci.* **424**, 271 (1999).
- <sup>24</sup>J. W. M. Frenken, B. J. Hinch, J. P. Toennies, and C. Wöll, *Phys. Rev. B* **41**, 938 (1990).